Polystyrene-grafted Carbon Fibers: Surface Properties and Adhesion to Polystyrene

ALEXANDER BISMARCK*
Department of Chemical Engineering & Chemical Technology
Polymer and Composite Engineering (PaCE)
Group in Materials Engineering & Technology
Imperial College London
South Kensington Campus
London, SW7 2AZ, UK

MATTHIAS PFAFFERNOSCHKE AND JÜRGEN SPRINGER
Technische Universität Berlin
Institut für Chemie
Fachgebiet Makromolekulare Chemie
Sekr. TC6, Straße des 17. Juni 135
D-10623 Berlin, Germany

ECKHARD SCHULZ
Laboratorium VI.2.1
Bundesanstalt für Materialforschung und – prüfung (BAM)
Unter den Eichen 87
D-12205 Berlin, Germany

ABSTRACT: It is highly desirable to improve attractive interactions between carbon fibers and unreactive thermoplastic matrices to the possible maximum. This could be achieved by a simple grafting process to create a covalently bonded interface or interlayer, which should result in cohesive interactions between the polymer-grafted fibers and the same matrix material, leading to a better adhesion strength in the obtained composite material. Here, we are describing the grafting of styrene onto unmodified and unsized carbon fibers via free-radical bulk polymerization in the presence of fibers. After grafting, the surface properties of the carbon fiber

*Author to whom correspondence should be addressed. E-mail: a.bismarck@imperial.ac.uk

0892-7057/05/04 0307–25 $10.00/0 DOI: 10.1177/0892705705049559

approach those of pure polystyrene which was proven by contact angle and zeta (ζ-) potential measurements. As indicated by the water contact angle, the carbon fiber surface becomes more hydrophobic. Scanning electron microscopy (SEM) provides evidence of grafted polymer. This simple procedure results in a continuous polystyrene coating. The fiber diameter increases significantly after polymer grafting. The adhesion and fracture behavior between the original and polystyrene-grafted carbon fibers to a polystyrene (VESTYRON®) matrix was characterized using the single-fiber pull-out test. There is a considerable increase in the measurable adhesion, i.e., the interfacial shear strength τ_{IFSS}, by almost 300% between the grafted fibers and polystyrene as compared to untreated original fibers. Two planes of interfacial failure could be distinguished; first in the fiber coating interface leading to lower interfacial shear strength and second in the PS-matrix–PS-coating interphase resulting in a higher interfacial shear strength. In addition to the improved adhesion, there are also clear differences in the pull-out behavior between the nongrafted and grafted fibers. After the initial debonding process corresponding to the maximal pull-out force is completed, the pull-out force is increasing again.

KEY WORDS: polystyrene, grafting, carbon fiber, contact angle, ζ-potential, adhesion, single-fiber pull-out test.

INTRODUCTION

OVER THE PAST four decades, fiber-reinforced polymer matrix composites have been intensively studied and have found many practical applications, from sporting equipment to aerospace, marine structures, and the oil industry. Despite all these achievements, there is still a need to improve certain fundamental properties, notably transverse and interlaminar performances, as well as resistance to environmental, chemical, and thermal damages. In addition, the through-life costs associated with composites are a significant factor during material selection for any given application. Understanding the physical and chemical mechanisms responsible for fiber–matrix adhesion, and the degradation as function of service time in given environments, is key to establishing predictable composite properties throughout the material's design life.

The desired mechanical properties of polymer composites are achieved only when the optimal stress transfer from the matrix material to the fiber reinforcement is guaranteed. In many cases, it is therefore necessary to modify the nonpolar carbon fiber surface to improve the adhesion between the polymeric matrix and carbon fibers. Many methods of surface modifications can be applied to carbon fibers, such as sizing, different wet chemical and dry oxidizing methods (i.e., boiling in oxidizing acids, plasma modifications, and electrochemical oxidations) [1–3]. The major drawback of oxidative carbon fiber treatments is often the loss in fiber tensile strength even though the adhesive behavior to the polymer matrix (mostly epoxy

resins) is improved. Commonly used oxidative surface treatments improve the fiber–matrix adhesion, for example, by increased polar interactions between surface oxides at the fiber surface and polar groups contained in the matrix. Other positive contributions to improved interfacial adhesion in composites are mechanical interlocking, attractive electrostatic interactions, and interdiffusion between a (flexible) polymeric interface on the carbon fiber surface and the matrix [4,5]. In thermoplastic composites, however, the fiber–matrix adhesion is generally poor because of the lack of strong covalent and/or ionic bonds between the inert thermoplastic resins and the reinforcing fibers [6]. The adhesion strength between reinforcing fibers and thermoplastics can be improved by forming covalent linkages between the fiber and the matrix by grafting a polymer of appropriate compatibility, molecular weight, and sufficient density on the fibers [7]. If the surface properties of the reinforcing fibers can be adjusted to match the properties of the matrix, the adhesive strength of the produced composite should mainly be determined by cohesion. Coated carbon fibers with a covalently bonded polymer should produce entanglements or in the case of polymer networks, interpenetrating networks between the surrounding polymer matrix and the polymeric interphase, immobilized on the carbon fibers.

Directly linked to the fiber–matrix adhesion is (generally) the impact performance of the composites [8]. Good fiber–matrix adhesion is required in order to achieve a high level of interlaminar shear strength. Many oxidative fiber treatments affect the fiber tensile strength, however, the application of matrix-compatible flexible polymeric 'interphases' will not have any damaging effect on the fiber strength. However, it was reported that it improves the interfacial adhesion between reinforcing (carbon) fibers and the matrix material [9,10], resulting additionally in an increased toughness, by absorbing the impact energy through deformation [11]. By changing the properties of the interlayer/coating, it should be possible to adjust the fiber–matrix adhesion, and therefore, to tailor the interface/interphase between reinforcement and matrix to the 'individual' requirements.

Several different possibilities exist to deposit coatings onto carbon fibers. However, if one is aiming to covalently attach polymeric coatings or interlayers to carbon fiber surfaces, there are only three methods available: plasma polymer deposition [12–17], electropolymerization or -deposition [8–11,18], and *in situ* chemical grafting reactions [19–24]. In earlier studies, we showed that it is possible to tune the carbon fiber chemistry and functionality and thereby their surface properties, i.e., hydrophilic/hydrophobic character, by grafting suited monomers such as methacrylic acid (MAA) [25], 2-(*N*,*N*-dimethylamino) ethyl methacrylate (DMAEMA) [26] and various liquid crystalline monomers [27,28] onto carbon fibers via

simple free radical bulk polymerization in the presence of the carbon fibers. The degree of grafting onto the surfaces can be adjusted by the amount of initiator used [29].

Here we describe our studies of grafting polystyrene onto carbon fibers to demonstrate the potential impact of covalently bonded interface or interlayer on the adhesion behavior between carbon fibers and a nonpolar thermoplastic matrix. The present study focuses on the characterization of the physical–chemical carbon fiber surface properties by ζ-potential and contact angle measurements. Moreover, the adhesion and fracture behavior between the PS-grafted carbon fibers and an industrially available PS-matrix (VESTYRON®) was characterized using the single-fiber pull-out technique.

EXPERIMENTAL PART

Grafting Reactions

For the experiments untreated, unsized polyacrylonitrile (PAN)-based high strength (HS) carbon fibers kindly supplied by SGL Carbon (Meitingen, Germany; Sigrafil C320.00A) were used.

The initiator azodiisobutyronitrile (AIBN), used in amounts of 0.5 and 2.0 mol%, was dissolved in styrene. The mixture was poured over the carbon fibers placed in a round-bottom flask. After rinsing the styrene carbon fiber mixture with nitrogen to replace oxygen, the reaction was started by heating the vessel to 55°C. The polymerization was terminated after 24 h. In order to remove all unreacted monomer and all nongrafted polymer from the fibers, the samples were continuously extracted with tetrahydrofurane (THF) for 7 days in a soxhlet and finally dried at 50°C, 1 mbar until constant weight was reached.

The polymer extracted from the fibers was used to determine the polymeric molecular weight distribution (MWD). The MWD was determined by gel permeation chromatography (GPC) in THF, using a WATERS 150C apparatus (Waters, Eschborn, Germany). Additionally, static light scattering (apparatus supplied by SLS Systemtechnik Hausen, Germany) was applied, to characterize the obtained 'bulk' polystyrenes.

In order to study the effect of the PS-grafting on the adhesion behavior between the modified fibers and PS, a commercially available material VESTYRON® 214 (Creanova Inc. (Hüls), Germany) was chosen as matrix material.*

*The mechanical, thermal, and electrical properties of the PS-matrix material used can be found at: http://www.matweb.com/SpecificMaterial.asp?bassnum=PHUM65&group=General accessed on 19.07.2003.

Surface Morphology

All treated fibers were analyzed by scanning electron microscopy (SEM) to show changes in the surface morphology. Fibers were investigated with a Hitachi S-2700 (Hitachi, Nissei Sangyo GmbH Ratingen, Germany) scanning electron microscope. Grafted fibers were sputtered with gold prior to microscopic analysis since the polymer is nonconducting.

Contact Angle Measurements

The modified Wilhelmy technique [30] was employed to determine the contact angles of fibers to water and to diiodomethane (p.a. grade purchased from MERCK-Schuchardt). The surface tension of the used test liquids were checked before measuring contact angles with the pendant drop method.

Due to the very small mass change (ca. 150 μg) of a monofilament during the measurement, five single fibers were placed parallel to each other in a distance of approximately 1–2 mm onto a measuring carrier. Weight changes were recorded using an ultramicroelectrobalance (Sartorius, Göttingen, Germany, accuracy = 0.1 μg, reproducibility = 0.2 μg) during the fiber immersion–emersion cycle at a stage velocity of 3 μm/s. The immersion and emersion of fibers into and from the test liquids were realized through a reversible elevator driven by a direct current (DC)-motor with a constant current source (Philips Power Supply Unit PE1507).

For calculating the contact angle θ, the fiber diameters d_f were estimated from scanning electron micrographs. Advancing θ_a and receding θ_r contact angles were calculated using the Wilhelmy equation from the mass changes, which were detected during the immersion and emersion of the fibers into and from the test liquid. No buoyancy slope was observed during the measurement. To check the reproducibility, all measurements were repeated at least six times for each sample with different fibers. All contact angle values reported here are the average values and the error values are the standard deviations.

To estimate γ_s of pure polystyrene (PS), 'static advancing' contact angles of the two test liquids on a polymer film were measured by sessile drop method applied in the Krüss DSA10 at room temperature (RT = 20°C). The measurements were taken immediately after the droplets were placed from above on the film surface. A microsyringe was used to form the droplets. At least 10 readings were taken for different drops placed on several spots of the surface. PS foils were obtained by pressing the pure polymer powder in a hot press for 2 min at 300 bar. The contact angle measurements were performed in an air conditioned room at 20°C. Solid surface tensions were calculated using the harmonic mean method introduced by Wu [36].

Zeta (ζ)-potential Measurements

ζ-Potentials were determined with the electrokinetic analyzer EKA (Anton Paar KG, Graz, Austria) based on the streaming potential method. Details of the ζ-potential measuring technique are reported elsewhere [31].

For the investigation of the concentration dependence of the ζ-potential, the EKA was filled with deionized (Millipore) water ($\kappa \leq 20\,\mu S/cm$). The cylindrical measuring cell was filled with ca. 2 g fiber; the cell was connected to the analyzer, rinsed with water, trapped air bubbles removed, and finally the measurement started. First the water-value of the ζ-potential was measured and subsequently the KCl concentration increased (using a digital burette from Fa. Brand, Wertheim, Germany). After each step, the whole system was rinsed thoroughly. The concentration was raised up to 10 mM KCl.

From the concentration dependence of the ζ-potential, it is possible to obtain information about the degree of interactions between the solid surface and the ions present in the solution, based on specific or electrostatic interactions. For most materials in contact with 1:1 electrolytes, the ζ-potential show a parabolic-like curve trend corresponding to the Stern theory, caused by the adsorption properties of the solid. Two characteristic parameters can be derived from this parabolic trend, the maximal ζ-potential ζ_{max} and the corresponding concentration value c_{max}. Knowing this values, it is possible to calculate the adsorption potentials (or adsorption free energies) Φ_+ of cations and Φ_- of anions on a solid surface combining the following equations:

$$2RT \ln c_{max} = \Phi_- + \Phi_+ \tag{1}$$

and

$$\Phi_- - \Phi_+ = 2F\zeta_{max} \tag{2}$$

R is the gas constant; F is the Faraday constant and T is the absolute temperature.

To measure the pH depending ζ-potential, the EKA was filled with a 1 mM KCl supporting electrolyte to keep the ion strengths constant. The cylindrical measuring cell was filled with approximately 2 g fiber; the cell was connected with EKA, rinsed with KCl-electrolyte solution, trapped air bubbles removed, and the measurement started. The pH-value varied in a range of 3–10 by adding 0.1 M HCl or KOH solution.

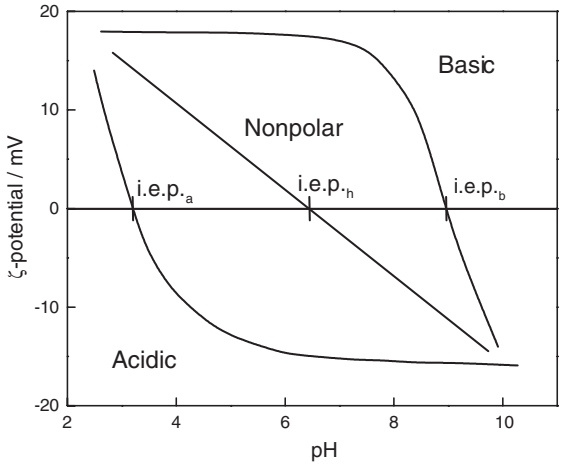

Figure 1. *Schematic picture of $\zeta = f(pH)$ for Brønstedt acidic and alkaline surface functional groups and for complete hydrophobic (i.e., nonpolar) surfaces.*

By measuring the pH dependence of the ζ-potential, the acidity or basicity of solid surfaces can be determined qualitatively. Figure 1 shows diagrammatically the ζ-potential as a function of pH for solids containing acid and basic surface functional groups and for an ideal hydrophobic material. The isoelectric point (iep) is a measure of the acidity or basicity of a solid surface, when the dissociation of surface groups is the dominant mechanism of the formation of the electrical double layer. If the iep is situated in the low pH-range then the solid surface exhibits an acidic character [32].

Single-fiber Pull-out Test

The samples for the pull-out tests were prepared in a special embedding machine, which allows an orientation perpendicular to the matrix surface at a defined embedded length [33]. A single fiber was partially embedded in a VESTYRON melt droplet on an aluminum sample carrier. A temperature of 260°C, which was well above the suggested processing temperature of 220°C, had to be chosen in order to ensure that the polymer flows easily and a single carbon fiber could be embedded into the melt droplet at a determined length between 50 and 200 μm. After embedding the fiber, the whole sample was cooled down to room temperature with nitrogen in about 2 min. After specimen preparation, the fiber diameters of all the specimens were measured using laser diffraction method [34].

The pull-out experiments were performed using a homemade apparatus with a high stiff frame to avoid energy storage in the free fiber length ($l_f = 30\,\mu m$) between the matrix surface and the clamping mechanism [35]. The fiber pull-out was performed at a constant speed of $0.2\,\mu m/s$ from the matrix using a controlled load cell. The pull-out load against displacement was recorded using a computer controlled plotter.

The apparent shear strength τ_{IFSS} was calculated from the maximum load F_{max} and fiber embedded area in the matrix using the mathematical relation,

$$\tau_{IFSS} = \frac{F_{max}}{\pi d L} \tag{3}$$

where L is the embedded length and d is the diameter of the fiber.

RESULTS AND DISCUSSION

Irrespective of the initiator concentration used (0.5 mol% AIBN: PS05; 2 mol% AIBN: PS2), the bulk polymerization of polystyrene yielded conversions of 35% after precipitating the reaction mixture in acetone. The results of the molecular weight determination are summarized in Table 1. A unimodal distribution was found for both materials, and the gel permeation chromatography (GPC) results indicate a rather similar degree of P_N. However, the dispersity of PS05 is slightly larger than that of PS2; $D = 1.81$ versus 1.76. The results of the light scattering experiments confirm these results.

Surface Morphology of Grafted Carbon Fibers – SEM Investigations

The scanning electron micrographs of the PS-grafted carbon fibers taken after THF-extraction to remove all loosely attached polymer chains show that the fibers increased in diameter (Figure 2(a) and (d); from 7 to

Table 1. Polymer characteristics – M_W(LS): Molecular mass determined by static light scattering, A_2(LS): Second osmotic virial coefficient, M_W(GPC): Molecular mass determined by gel permeation chromatography, P_N(GPC): Degree of polymerization, determined permeation chromatography, respectively, D: polydipersity = M_W/M_N.

Material	M_W(LS) (g/mol)	A_2(LS) (mol mL/g)	M_W(GPC) (g/mol)	M_N(GPC) (g/mol)	P_N(GPC)	D
PS05	2.01×10^5	7.32×10^{-4}	1.87×10^5	1.04×10^5	1000	1.81
PS2	1.81×10^5	5.29×10^{-4}	1.61×10^5	0.91×10^5	900	1.76

approximately 9 μm), compared to the original fiber (around 7 μm). Since the scanning electron micrographs represent only a small picture of the overall fiber sample, a laser diffraction method was used to measure and verify change of the fiber diameters. The results are summarized in Table 3. The fiber diameter and, therefore, the coating thickness increases with increasing initiator amount used for the grafting process. The higher the amount of initiator used, the more free polymer radicals are present, and therefore the probability increases that growing but shorter polymer radicals attach themselves to the carbon fiber surfaces resulting in a more perfect and denser coating.

The striations present at the surface of the original fibers (Figure 2(a)) are due to the manufacturing process (extrusion and stretching) of PAN-precursors fibers. No obvious significant differences between both grafted fibers (0.5 and 2 mol% AIBN, respectively) can be observed. However, the electron backscattering micrographs of the PS-grafted fibers looking at the fiber cross sections (Figure 2(b) and (c) 0.5 mol% and 2 mol%, respectively) highlight some differences. The PS coating appears as a

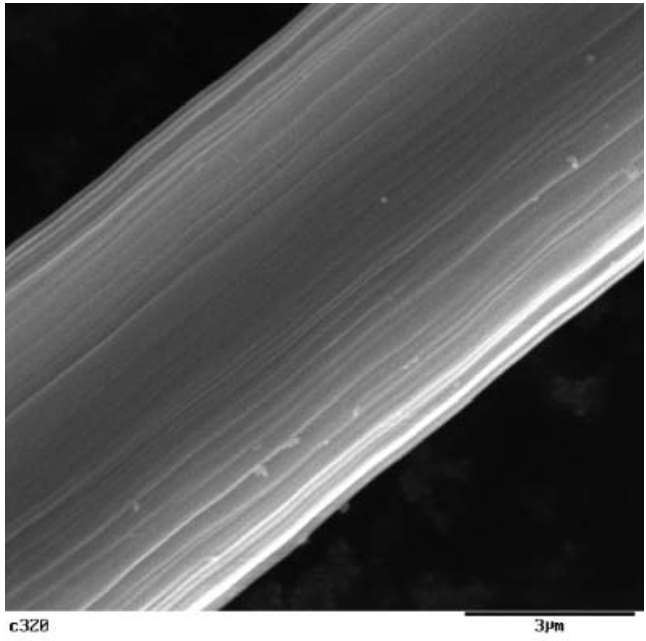

(a)

Figure 2. *Scanning electron micrographs of a nongrafted (original) carbon fiber (a), with 0.5 mol% (b) and with 2.0 mol% AIBN PS-grafted carbon fiber (cross section (c), and overall micrograph (d)).*

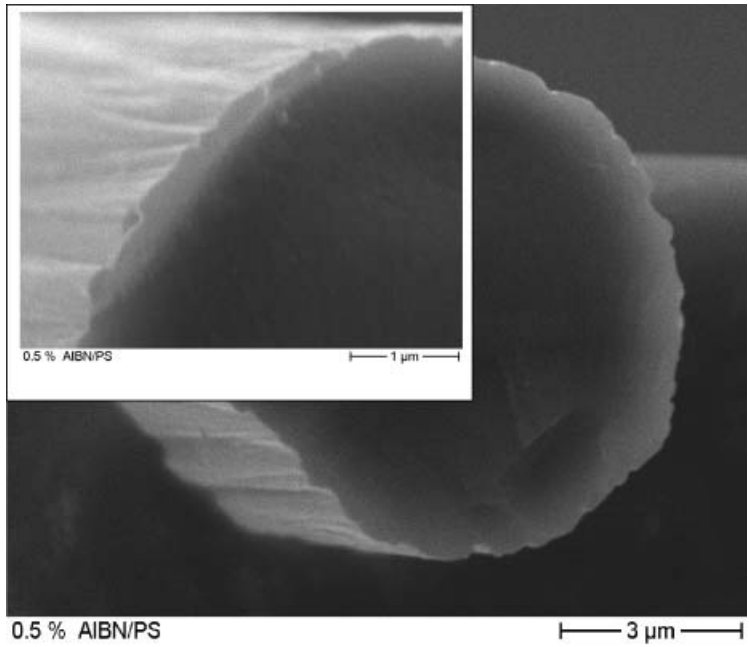

(b)

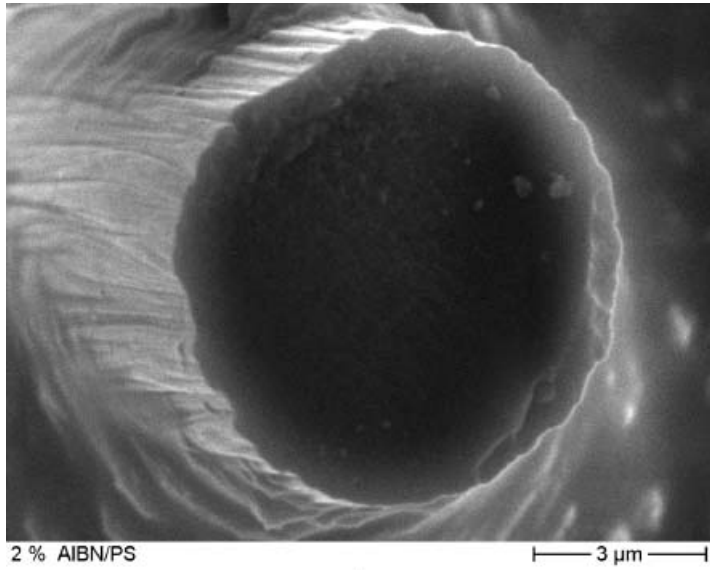

(c)

Figure 2. *Continued.*

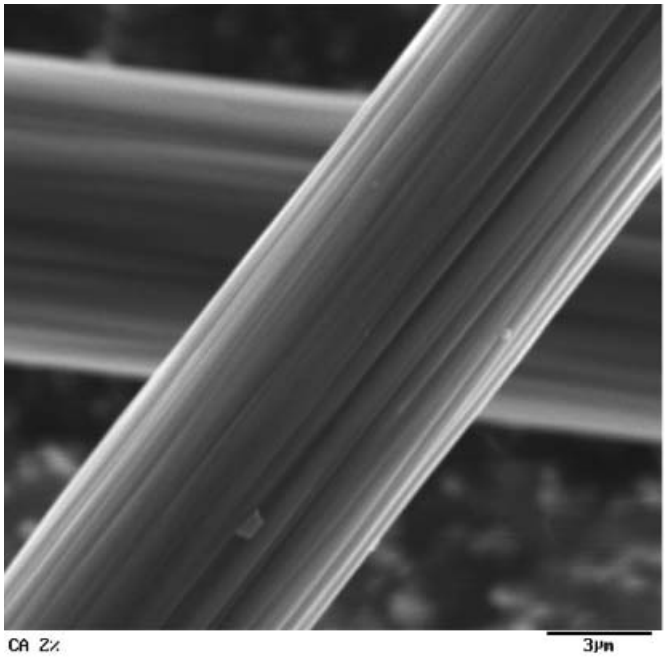

(d)

Figure 2. *Continued.*

brighter edge all around the carbon fiber core. The only apparent difference between the fibers grafted using 0.5 and 2 mol% initiator seems to be, that the fibers 2 mol% PS-grafted fibers have not a smooth coating as the 0.5 mol% PS-grafted fibers.

Contact Angle Measurements

The mean values of the advancing water contact angles θ_a (see Table 2) increase with increasing coating thickness, i.e., increasing initiator amount used. The contact angle values approach the value measured for PS. The contact angle hysteresis, defined as the difference between θ_a and the receding contact angle θ_r, seems to be unaffected by grafting polymer chains to the fiber surfaces. The hysteresis is usually attributed to the chemical heterogeneity and roughness of probed surfaces. Probably more remarkable is the decrease of θ_a measured versus diiodomethane jumping toward the value of PS. In case of the nonpolar test liquid diiodomethane, no contact angle hysteresis could be observed indicating the prevailing dispersive interactions. This becomes also obvious in the decreasing surface polarity

Table 2. Advancing θ_a and receding θ_r contact angles measured vs water and DIM, polar γ^p and dispersive γ^d component of the solid surface tension γ and the surface polarity $X^p = \gamma^p/\gamma$.

Material	$\theta_a(H_2O)$ (°)	$\theta_r(H_2O)$ (°)	θ_a(DIM) (°)	θ_r(DIM) (°)	γ^p (mN/m)	γ^d (mN/m)	γ (mN/m)	X^p
0*	82.5 ± 2.9	56.3 ± 3.1	49.9 ± 3.2	47.7 ± 1.9	8.2 ± 1.3	35.6 ± 1.6	43.8 ± 2.8	0.19
0.5*	84.9 ± 2.2	69.9 ± 2.4	41.2 ± 2.0	40.2 ± 2.3	6.5 ± 0.9	39.6 ± 0.9	46.1 ± 1.8	0.14
2.0*	86.4 ± 2.2	58.1 ± 2.7	41.0 ± 0.9	41.5 ± 1.2	5.9 ± 0.9	45.6 ± 0.4	45.6 ± 1.3	0.13
PS**	85.5 ± 3.8	–	30.2 ± 1.6	–	5.6 ± 1.5	44.3 ± 0.6	49.9 ± 2.1	0.11

*Carbon fiber grafted with *x* mol% AIBN; **PS foil.

Table 3. Fiber diameter d_f of the original and PS-grafted carbon fibers as well as the apparent interfacial shear strength τ_{IFSS} and force C required for the collar (fractured wetting cone) formation of fibers embedded in a VESTYRON® PS matrix.

Carbon fiber	d_f (μm)	τ_{IFSS} (MPa)	C (mN)
0	7.34 ± 0.25	4.6 ± 1.8	43 ± 6
0.5	7.55 ± 0.59	6.5 ± 3.4	25 ± 12
2.0	8.48 ± 0.39	13.7 ± 6.4	12 ± 18

of the fibers. The surface tensions (Table 2), calculated from θ_a values reflecting the characteristics of the lower energy part of a solid [36], also clearly approach the value of PS. These values are in good agreement to published results [36], and indicate that the carbon fiber surface behaves more and more polystyrene-like by increasing the amount of AIBN and thereby the coating thickness.

ζ-Potential Measurements

Every measurement of concentration- or pH-dependent ζ-potentials need a well-defined starting point. This point depends on the time that a particular system requires for 'equilibration' and is approached by a long-time measurement. The main results of the ζ-potential measurements are summarized in Table 4. The concentration dependence of the ζ-potential (Figure 3) of all investigated carbon fibers shows a parabolic curve-like trend. The value of the ζ-potential measured in pure water almost doubles for the PS-grafted carbon fibers, which indicates a change in the ratio of ion-to-water adsorption. Since the surface of the modified carbon fibers becomes slightly more hydrophobic, as shown by contact angle

Table 4. Results of the ζ-potential measurements; ζ_o, ζ_∞ from the $\zeta = f(t)$, i.e.p. and $\zeta_{plateau}$ from $\zeta = f(pH)$-function and the in surface conductance corrected ζ_{max} and c_{max} from $\zeta = f(t)$ as well as the adsorption potentials Φ_- for Cl^- and Φ_+ for K^+ ions.

Material	i.e.p.	$\zeta_{plateau}$ (mV)	ζ_{max}(CSC) (mV)	c_{max} (mmol/l)	Φ_- (kJ/mol)	Φ_+ (kJ/mol)
0*	4.2	-26.0 ± 1.2	-28.4 ± 0.2	6	-15.4 ± 0.1	-9.9 ± 0.1
0.5*	3.8	-36.6 ± 0.6	-29.8 ± 0.5	0.8	-20.4 ± 0.2	-14.7 ± 0.1
2.0*	4.1	-49.1 ± 1.0	-41.6 ± 0.4	0.8	-21.6 ± 0.2	-13.5 ± 0.3
PS**	4.0	-40.4 ± 5.0		Not measurable***		

*Grafted with *x* mol% AIBN; **'pure' polystyrene foil; ***due to problems to accurately measure the electrical resistance at low electrolyte concentration.

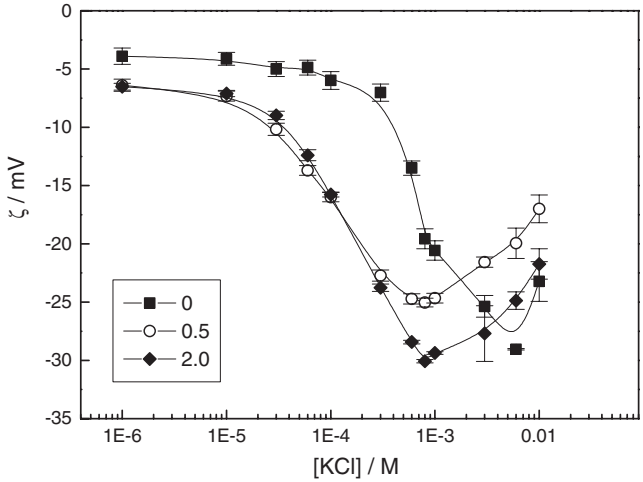

Figure 3. *Concentration dependence of the ζ-potential of 'original' nongrafted and polystyrene-grafted carbon fibers.*

measurements, the adsorption of water is less favorable. The formation of the electrochemical double layer strongly depends on the adsorption of ions which occurs in competition with water adsorption [37], i.e., causing the more negative ζ_{max}-values of the PS-grafted carbon fibers compared to untreated carbon fibers [37].

The maximum ζ-potential value (ζ_{max}) for the grafted carbon fibers shifts to higher ζ-potentials and the corresponding concentration value c_{max} to lower values as compared to the original fibers. The adsorption free energies of Cl^- and K^+ (Table 4) calculated using Equations (1) and (2) from the ζ-potential values corrected for surface conductance show that Cl^- is adsorbed in excess on all carbon fiber surfaces. This behavior is expected,

since anions are bigger and, therefore, easier to polarize and less hydrated so that they have the greater tendency to participate at an electrolyte–solid interface, especially when the surface is hydrophobic [38].

The ζ-potentials measured as a function of pH $\zeta = f(\text{pH})$ for all carbon fibers, original and grafted, and for the pure PS show a distinct plateau region at higher pH values (Figure 4). The unmodified carbon fibers (0) contain due air contact at elevated temperatures during the manufacturing process or long-time exposure to air-oxygen [39], acidic (carboxyl- or hydroxyl-) surface functional groups (CA surface composition obtained from XPS-spectra: C: 93.2 atomic %, O: 4.6 atomic %, N: 1.2 atomic %, and Na: 0.6 atomic %) which were formed with unsaturated carbon atoms at the basal plane edges. At lower pH values, the adsorption of protons, which are potential determining ions (pdi), is the predominant mechanism. This leads to a reversal of the ζ-potential for all fibers. A similar $\zeta = f(\text{pH})$ was measured for PS indicating a prevailing acidic surface character, explaining the rather similar values of the iep for the carbon fibers 0, 0.5, and 2.0. A clear difference between the original carbon fibers and PS is the difference in the ζ_{plateau}-values at pH > 7. PS has a much smaller ζ_{plateau}-value. The ζ_{plateau}-values of polymeric materials also affected by the hydrophilic/hydrophobic character (compare with contact angle data) as described previously for textile fibers [40], the more hydrophilic a solid, the higher the competition between water and ion adsorption at its surface. Therefore, the higher the surface coverage of the carbon fibers by PS, the higher is the

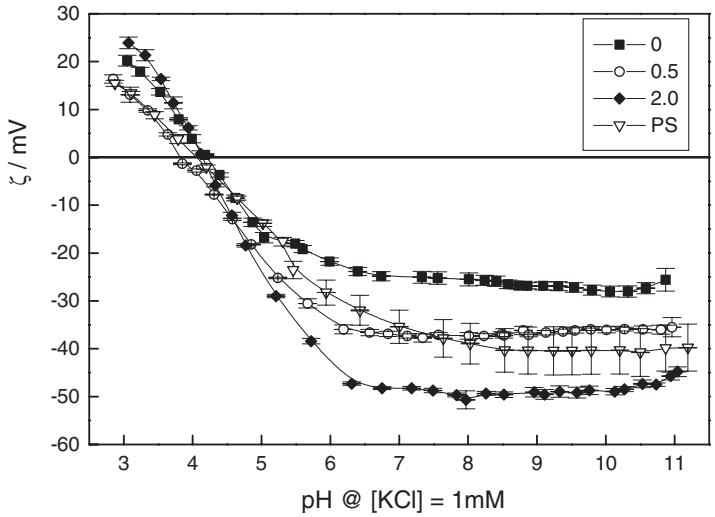

Figure 4. *pH-dependent ζ-potential of 'original' nongrafted and polystyrene-grafted carbon fibers and of 'pure' polystyrene (foils) measured in 1 mM KCl supporting electrolyte.*

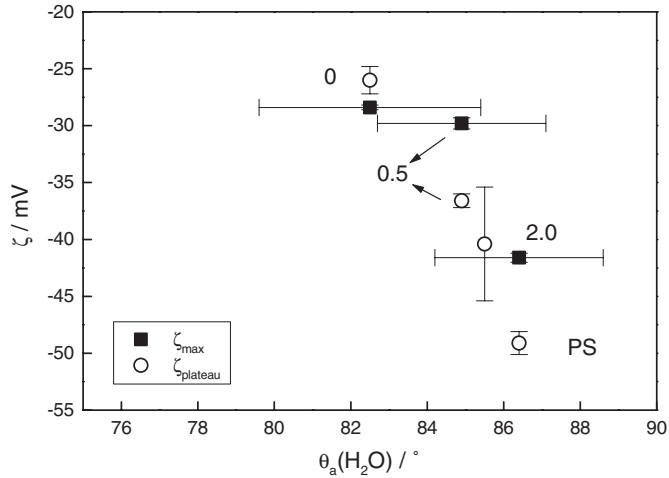

Figure 5. *ζ-Potential ($\zeta_{plateau}$ and ζ_{max}) as function of advancing water contact angles $\theta_a(H_2O)$.*

measured ζ_{plateau}-value. A connection between $\zeta_{\max}$ [41] but also the ζ_{plateau}-values [42] with the advancing water contact angles θ_a could be observed (Figure 5).

The larger errors of the pH-depending ζ-potentials of the PS foil are caused because a different measuring setup had to be used. The ζ-potentials of polymer foils were measured with a rectangular cell in a narrow channel (channel geometry: thickness $\approx 150\,\mu\text{m}$, width $\approx$ mm, length ≈ 73 mm). In such an arrangement, surface imperfections, or imperfect channels will result in relatively big differences of the streaming potential measured in the different directions (we call it 'left/right dependence'). Nevertheless, the ζ_{plateau}-values of the PS-grafted carbon fibers correspond reasonably well to the value of the 'pure' PS.

Adhesion Behavior between Grafted Carbon Fibers and a PS Matrix

The dependence of the apparent interfacial shear strength τ_{IFSS} on the embedded fiber length L_e allows to distinguish between brittle and ductile fracture behavior between the fiber–matrix interphase. A relatively amorphous boundary layer would result in ductile failure, whereas crystalline structures at the fiber–matrix interface cause increased adhesion to the fiber that leads to brittle fracture during the single-fiber pull-out test [43].

The lines in the plot of the apparent shear strength as function of embedded fiber length (Figure 6) should be taken only as a trend indicator,

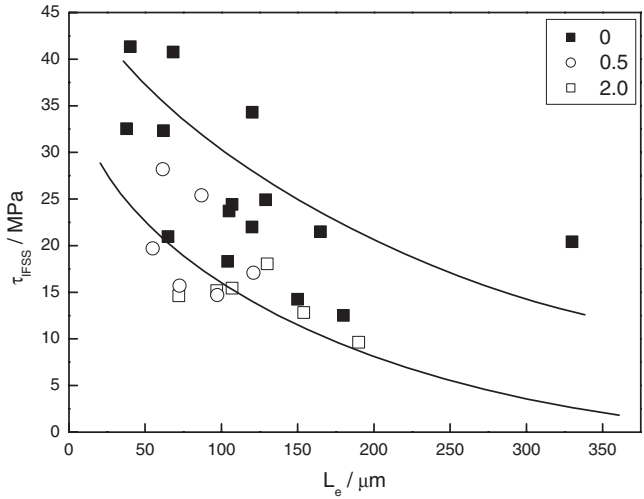

Figure 6. *Apparent interfacial shear strength τ_{IFSS} of the unmodified 'original' fiber (0) and the PS-grafted fibers (0.5 and 2.0) as function of the embedded fiber length.*

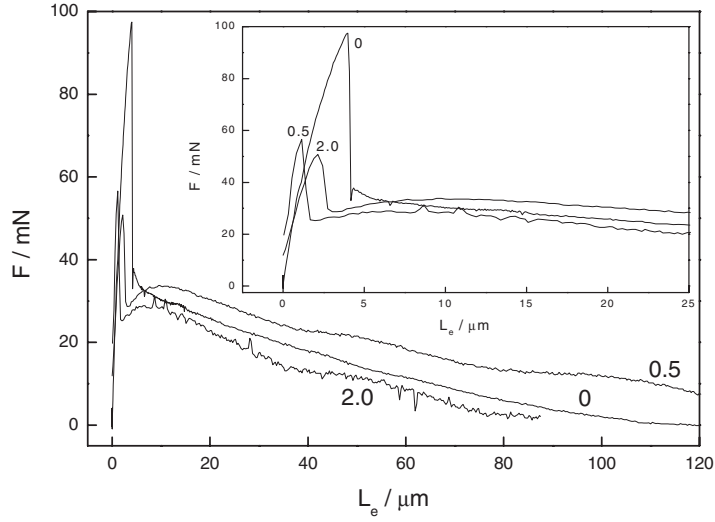

Figure 7. *Fiber pull-out force–displacement curves of the unmodified, pristine (0), and PS-grafted fibers (0.5 and 2.0) embedded in Vestyron Polystyrene.*

and they do not represent any data fitting. All measured values for all investigated carbon fibers including the PS-grafted fibers follow a common, but scattered trend. An apparent interfacial shear strength that decreases with increasing embedded fiber length indicates a brittle failure of

the fiber–matrix interface [43], which was observed for the original as well as the PS-grafted carbon fibers. Initially the load increases linearly corresponding to a perfect fiber–matrix interface (Figure 7). However, with increasing load stable interfacial debonding occurs and a crack begins to form causing the deviation from linearity. After a critical crack length, the failure process becomes unstable leading to sudden and complete debonding and the pull-out forces drops sharply to a much lower level which is governed by the frictional sliding of the fiber in the matrix [44]. In case of the untreated fibers, the pull-out force is linearly decreasing with increasing pull-out due to the reduced contact area. However, for the grafted fiber the pull-out force in the friction region starts to increase again and another, but local force maximum is observed (Figure 7). The increase in pull-out force after debonding could be caused by polymer relaxation processes, i.e., resolving entanglements between the PS grafted to the fibers and the surrounding matrix.

Figure 8 presents the measured maximum pull-out forces between the fibers and the PS as a function of the embedded fiber area A_e. It can be seen that the experimental data points are quite scattered. The large scatter of the results is due to the fact, that the measured maximum force is affected by thermal shrinkage, interfacial flaws, and the friction in the debonded regions [45]. Moreover, in case of the single-fiber composites, the formation of collars, fractured wetting cones, could be observed. As can be seen from the

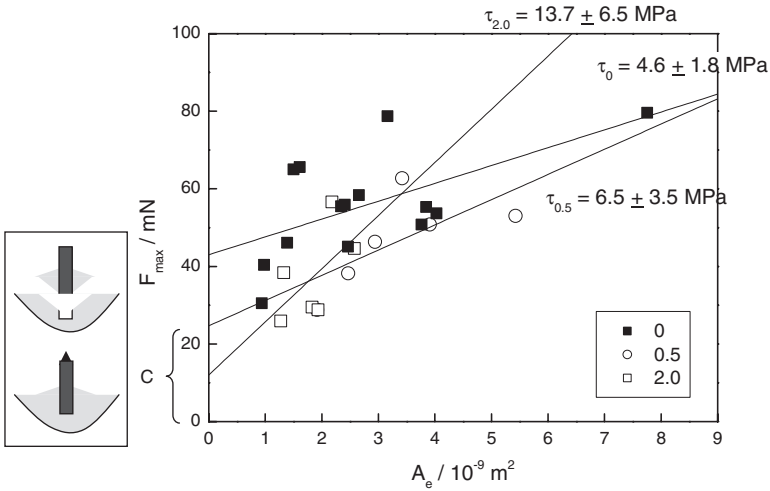

Figure 8. *The maximum pull-out force F_{max} of the unmodified, original fiber (0) and the PS-grafted fibers (0.5 and 2.0) as function of the embedded fiber area. The resulting intercept C is due to the formation of a collar (fractured wetting cone) still attached to the fiber (see also Figures 9 and 10 (c), (d)) after being pulled out of the matrix, which is diagrammatically shown in the insert.*

scanning electron micrographs taken of the tested single-fiber composite samples (Figures 9–11), two different failure processes can be clearly distinguished. First, the fiber–grafted PS-coating interface failed during the pull-out process; a clean fiber (Figure 10(a)) was pulled out of the grafted PS-coating, which is still 'embedded' in the PS matrix (Figure 10(b)). Second, other fibers, adhering stronger to the PS matrix, show different sized collars around them and have also still some matrix material adhering to the fibers (Figures 10(c), (d) and 11(a), (b)). These different interfacial failures (and maybe mixed failure modes) might be the cause for the big scatter in the determined interfacial shear strength values. None of the linear

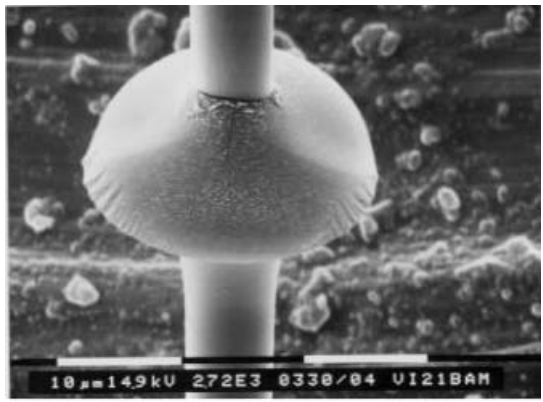

(a)

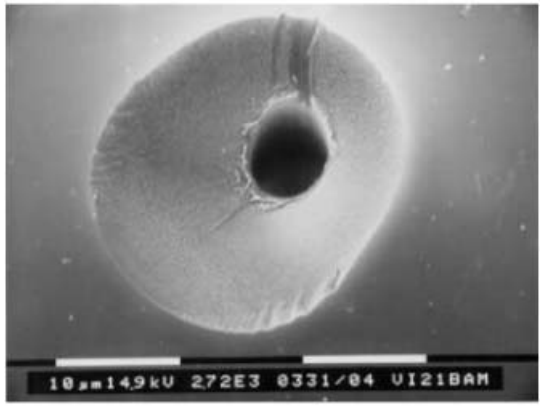

(b)

Figure 9. *Scanning electron micrograph of a single 'original' carbon fiber taken after the pull-out experiment showing a collar of fractured PS matrix around a clean pulled-out fiber (a) and the corresponding matrix droplet from which the fiber was pulled out (b).*

fits to the experimental data is passing through the origin of the graph. Subramanian et al. [46] described a similar pull-out behavior. The relationship that describes our data is therefore:

$$\tau = \frac{F}{\pi dL} + C$$

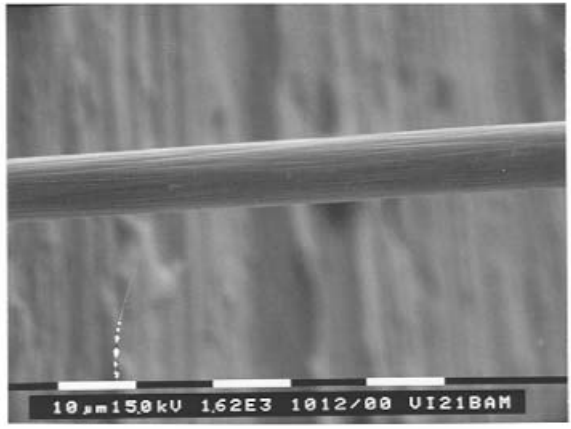

(a)

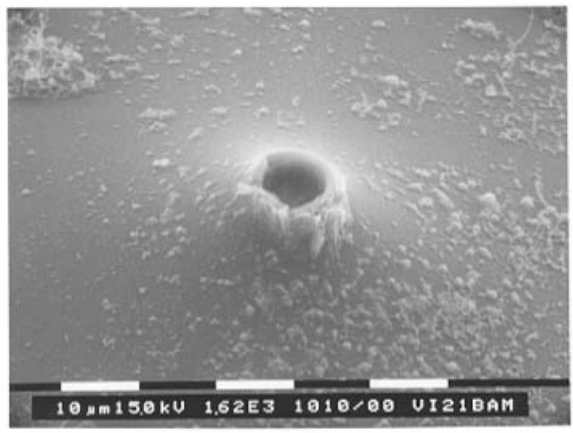

(b)

Figure 10. *Scanning electron micrograph of a single fiber composite with 0.5 mol% PS grafted carbon fiber taken after the pull-out experiment showing (i) a 'clean' (decoated) fiber pulled out (a) from the PS matrix (b) and (ii) a fiber with a collar of fractured matrix (c) and the corresponding matrix droplet from which the fiber was pulled out (d).*

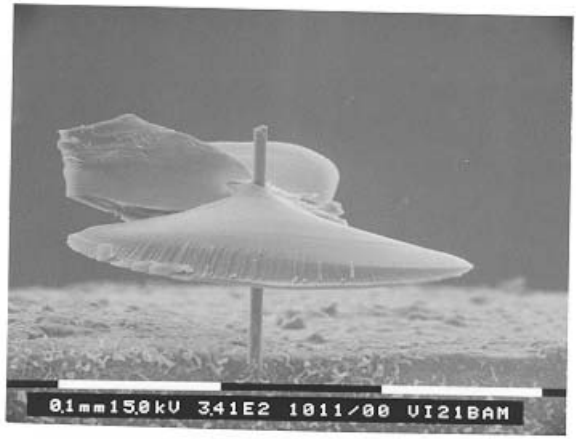

(c)

(d)

Figure 10. *Continued.*

C reflects the force required to fracture the matrix material leading to the formation of collars adhering to the fiber. This force C, required to fracture the PS matrix to form a collar, is needed to be expended before the fiber pull-out can occur. The values of C and the corresponding standard deviations are listed in Table 3. Again, the scatter of the determined C-values is extremely large. This is due to the fact that different sized collars were formed and sometimes even 'clean' fibers were pulled out of the matrix.

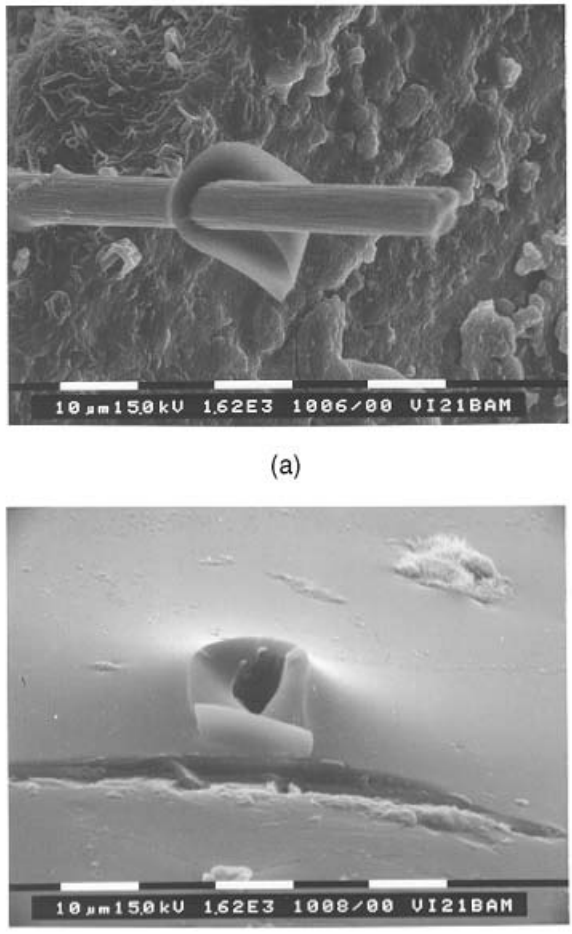

Figure 11. *Scanning electron micrograph of a single fiber composite with 2.0 mol% PS-grafted carbon fiber taken after the pull-out experiment showing a fiber with a collar of fractured matrix (a) and the corresponding matrix droplet from which the fiber was pulled out (b).*

Somehow, surprisingly the force needed to form a collar seems to decrease with increasing amount of polymer grafted to the fiber.

Even though the experimental scatter is large, distinct trends between the original and unmodified fibers can be seen. The apparent interfacial shear strength τ_{IFSS}, corresponding to the slope of the pull-out force fiber area curve [46], was determined by a linear fit to the measured data. The results

are summarized in Table 3. The mean apparent interfacial shear strength, as a measure of practical adhesion, increases with increasing amount of grafted PS. The increasing amount of grafted material is evidenced by the increasing fiber diameter.

CONCLUSIONS

It has been shown that grafting of styrene onto carbon fiber surfaces can be performed easily by free radical bulk polymerization in the presence of carbon fibers. The amount of initiator used for the grafting procedure affects the amount of the polymer grafted to the fibers. The higher the amount of initiator used, the more free (polymer) radicals are present, and therefore the probability increases that a growing polymer radical attaches itself to the carbon fiber surface. Contact angle measurements as well as ζ-potential measurements showed that the surface properties of the grafted fibers become more PS-like. The ζ-potential plateau values obtained from the $\zeta = f(\text{pH})$ as well as $\zeta = f([\text{KCl}])$ correlate with the advancing water contact angles. As can be seen from the ζ-potential measurements, a high degree of compatibilization between the PS-grafted carbon fibers and a PS matrix can be expected. Both the PS-grafted fibers and the matrix show within the experimental error, a similar behavior. Therefore, good interaction cohesion and entanglements between the grafted PS and the matrix can be expected.

It is highly desirable to improve adhesion between carbon fibers and a surrounding polymer matrix in particular for thermoplastics to the possible maximum. As demonstrated using the single-fiber pull-out tests, even though the experimental scatter is large, there is a considerable increase in the measurable adhesion, i.e., the interfacial shear strength τ_{IFSS}, by almost 300% between the grafted fibers and a commercial PS matrix as compared to untreated original fibers. However, two clear 'planes' of failure can be distinguished; first in the fiber coating interface leading to lower interfacial shear strength and second in the PS matrix–PS coating interface resulting in higher shear strength. In addition to the improved adhesion, there are also clear differences in the pull-out behavior between nongrafted and grafted fibers. After the initial debonding process corresponding to the maximal pull-out force is completed, the pull-out force is increasing again, which could be due to relaxation processes occurring in the coating–matrix–fiber interface, i.e., dissolving polymer–polymer entanglements. Such a behavior might contribute positively to the overall properties of fiber-reinforced polymer composites.

ACKNOWLEDGMENTS

Special thanks to Ute Wild (Fritz Haber Institut der Max-Planck-Gesellschaft Berlin) for recording the XPS of the unmodified carbon fiber, Jörg Nissen (Zentraleinrichtung Elektronenmikroskopie der TU-Berlin, ZELMI) for taking the SEMs and Martina Bistritz (BAM-Berlin) for performing the pull-out experiments. Furthermore, we are indebted to Hannelore Oehlert, Manuela Krüger, and Annegret Niehenke-Mölders (formerly Institut für Technische Chemie of the TU-Berlin) for the polymer characterization.

We would also like to thank the referees for their most appreciated comments that helped to improve the manuscript.

REFERENCES

1. Peng, J.C.M., Donnet, J.-B. and Rebouillat, S. (1998). Surface Treatment of Carbon Fibers, In: Donnet, J.-B., Wang, T.K., Rebouillat, S. and Peng, J.C.M. (eds), *Carbon Fibers*, **3rd edn**, Marcel Dekker, New York.
2. Kim, J.-K. and Mai, Y.-W. (1998). Surface Treatments of Fibers and Effects on Composite Properties, In: *Engineered Interfaces in Fiber Reinforced Composites*, Elsevier, Amsterdam.
3. Luo, S. and van Ooij, W.J. (2002). Surface Modification of Textile Fibers for Improvement of Adhesion to Polymeric Matrices: A Review, *J. Adhesion Sci. Technol.*, **16**: 1715.
4. Le Bonheur, V. and Stupp, S.I. (1994). Coupling Carbon Fibers to Epoxy Matrices with Grafted Side-Chain Liquid-Crystal Polymers, *Chem. Mater.*, **6**: 1880.
5. Jacobasch, H.-J., Freitag, K.-H., Panzer, U. and Grundke, K. (1991). Charakterisierung und Modifizierung der Oberflächeneigenschaften von Fasern für Verbundwerkstoffe, *Chemiefasern/Textilindustrie*, **93**: 39.
6. Raghavendran, V.K. and Drzal, L.T. (2002). Fiber-matrix Interfacial Adhesion Improvement in Carbon Fiber-Bisphenol-A Polycarbonate Composites by Polymer Grafting, *J. Adhesion*, **78**: 895.
7. Drzal, L.T. and Raghavendran, V.K. (2003). Adhesion of Thermoplastic Matrices to Carbon Fibers: Effect of Polymer Molecular Weight and Fiber Surface Chemistry, *J. Thermoplast. Composite Mater.*, **16**: 21.
8. Subramanian, R.V. and Crasto, A.S. (1986). Electrodeposition of a Polymer Interphase in Carbon-Fiber Composites, *Polym. Composites*, **7**: 201.
9. Subramanian, R.V. (1980). Electrochemical Polymerization and Deposition on Carbon Fibers, *Pure Appl. Chem.*, **52**: 1929.
10. Iroh, J.O. and Jordan, K.M.S. (2000). Mechanical Properties of Carbon Fibre/PMR-15 Composites Containing Thermoplastic Polymide Interphase Coatings, *Surf. Engin.*, **16**: 303.
11. Crasto, A.S., Own, S.H. and Subramanian, R.V. (1988). The Influence of the Interphase on Composite Properties – Poly(Ethylene-co-Acrylic Acid) and Poly(Methyl Vinyl Ether-co-Maleic Anhydride) Electrodeposited on Graphite Fibers, *Polym. Composites*, **9**: 78.
12. Li, Z.F. and Netravali, A.N. (1992). Surface Modification of UHSPE Fibers Through Allylamine Plasma Deposition: 2. Effect on Fiber and Fiber Epoxy Interface, *J. Appl. Polym. Sci.*, **44**: 333.
13. Waldman, D.A., Zou, Y.L. and Netravali, A.N. (1995). Ethylene Ammonia Plasma Polymer Deposition for Controlled Adhesion of Graphite Fibers to PEEK: 1. Characterization of Plasma Formed Polymers, *J. Adhesion Sci. Technol.*, **9**: 1475.

14. Zou, Y.L. and Netravali, A.N. (1995). Ethylene Ammonia Plasma Polymer Deposition for Controlled Adhesion of Graphite Fibers to PEEK: 2. Effect on Fiber and Fiber/Matrix Interface, *J. Adhesion Sci. Technol.*, **9**: 1505.
15. Dilsiz, N., Erinç, N.K., Bayramli, E. and Akovali, G. (1995). Surface-Energy and Mechanical-Properties of Plasma-Modified Carbon-Fibers, *Carbon*, **33**: 853.
16. Dilsiz, N. (2000). Plasma Surface Modification of Carbon Fibers: A Review, *J. Adhesion Sci. Technol.*, **14**: 2000.
17. Yamada, K., Yamane, H., Kumada, K., Tanabe, S. and Kajiyama, T. (2003). Plasma-graft Polymerization of a Monomer with Double Bonds onto the Surface of Carbon Fiber and its Adhesion to a Vinyl Ester Resin, *J. Appl. Polym. Sci.*, **90**: 2415.
18. Bismarck, A., Menner, A., Kumru, M.E., Saraç, A.S., Bistritz, M. and Schulz, E. (2002). Poly(carbazole-co-acrylamide) Electrocoated Carbon Fibers and their Adhesion Behavior to an Epoxy Resin Matrix, *J. Mater. Sci.*, **37**: 461.
19. Brie, M., Cazard, J., Lang, F.-M. and Riess, G. (1971). Greffage de poymères Ssur fibres de carbone, *Bull. Inform. Sci. Techn. Commis. Energ. At.*, **155**: 31.
20. Brié, M. and Le Dressus, C. (1973). Grafting of Polymers on Carbon Fibres (Greffage de poymeres sur fibres de carbone), *Fibre Sci. Technol.*, **6**: 47.
21. Koschinski, I. and Reichert, K.H. (1988). Preparation of Carbon-Fiber Reinforces Poly (Phenylene Sulfide) by In-Situ Polymerization, *Makromol. Chem. Rapid*, **9***:* 291.
22. Bhama, S. and Stupp, S.I. (1990). Grafting of a Liquid-Crystal Polymer on Carbon-Fibers, *Polym. Engin. Sci.*, **30**: 603.
23. Raghavendran, V.K. and Drzal, L.T. (2002). Grafting of Bisphenol-A Polycarbonate and Polymethyl Methacrylate on to the Surface of Carbon Fibers via Anionic Polymerization, *Composite Interfaces*, **9**: 1.
24. Yan, W.X., Han, K.Q., Qin, L.L. and Yu, M.H. (2004). Study on Long Fiber-reinforced Thermoplastic Composites Prepared by In Situ Solid-state Polycondensation, *Appl. Polym. Sci.*, **91**: 3959.
25. Bismarck, A., Pfaffernoschke, M. and Springer, J. (1999). Grafted Carbon Fibers and their Physico-chemical Properties; Part I: Grafting of Methacrylic Acid onto Carbon Fibers, *J. Appl. Polym. Sci.*, **71**: 1175.
26. Bismarck, A., Pfaffernoschke, M., Selimović, M. and Springer, J. (1998). Grafted Carbon Fibers and their Physico-chemical Properties. Part II. Grafting of Liquid Crystalline Methacrylic Monomers onto Carbon Fibers and the Influence of an Applied Voltage to the Carbon Fiber Embedded in a Liquid Crystalline Matrix, *Colloid Polym. Sci.*, **276**: 1110.
27. Bismarck, A., Pfaffernoschke, M., Song, B. and Springer, J. (1999). Grafted Carbon Fibers and their Physico-chemical Properties. Part II. Grafting of Liquid Crystalline Methacrylic Monomers onto Carbon Fibers and the Influence of an Applied Voltage to the Carbon Fiber Embedded in a Liquid Crystalline Matrix, *J. Appl. Polym. Sci.*, **71**: 1893.
28. Selimović, M., Bismarck, A., Pfaffernoschke, M. and Springer, J. (1999). Grafted Carbon Fibers and their Physico-chemical Properties; Part IV: Grafting of Cyano-Biphenyl Containing Liquid-Crystalline Monomers onto Modified Carbon Fibers, *Acta Polymerica*, **50**: 156.
29. Donnet, J.B., Papirer, E. and Vidal, A. (1975). In: Walker, P.I. and Thrower, P.A. (eds), *Chemistry and Physics of Carbon*, Marcel Dekker, New York.
30. Collins, G.E. (1947). A Surface Tension Method for Measuring the Perimeters of Fibres and the Contact Angles of Liquids against Fibers, *J. Textile Inst.*, **38***:* T73.
31. Jacobasch, H.-J., Simon, F., Werner, C. and Bellmann, C. (1996). Elektrokinetische Meßmethoden: Grundlagen und Anwendungen, *Technisches Messen*, **63**: 447.
32. Mäder, E., Grundke, K., Jacobasch, H.-J. and Wachinger, G. (1994). Surface, Interphase and Composite Property Relations in Fiber-reinforced Polymers, *Composites*, **25**: 739.

33. Hampe, A. and Marotzke, C. (1992). Adhesion of Polymers to Reinforcing Fibers, *Polym. Intern.*, **28**: 313.
34. Meretz, S., Linke, T., Schulz, E., Hampe, A. and Hentschel, M. (1992). Diameter Measurement of Small Fibers – Laser Diffraction and Scanning Electron-Microscopy Techique Results do not Differ Systematically, *J. Mater. Sci. Lett.*, **11**: 1471.
35. Hampe, A., Kalinka, G., Meretz, S. and Schulz, E. (1995). An Advanced Equipment for Single-Fiber Pull-Out Test Designed to Monitor the Fracture Process, *Composites*, **26**: 40.
36. Wu, S. (1982). *Polymer Interface and Adhesion*, Marcel Dekker, New York.
37. Jacobasch, H.-J. (1984). *Oberflächenchemie faserbildender Polymerer*, Akademie Verlag, Berlin.
38. van Wagenen, R.A., Coleman, D.L., King, R.N., Triolo, P., Brostrom, L., Smith, L.M., Gregonis, D.E. and Andrade, J.D. (1981). Streaming Potential Investigations – Polymer Thin-Films, *J. Colloid Interface Sci.*, **84**: 155.
39. Mattson, S.J. and Mark, Jr., H.B. (1971). *Activated Carbon; Surface Chemistry and Adsorption from Solution*, Marcel Dekker, New York.
40. Ribitisch, V. and Stana-Kleinschenk, K. (1997). Characterization of Textile Fiber Surfaces by Streaming Potential Measurements. Contribution at International Zetapotential Workshop, Graz.
41. Kuehn, N. (1985). Elektrokinetische Erscheinungen im Offsetdruck, In: *Symposium Proceedings, Elektrokinetische Erscheinungen '85*, Institut für Technologie der Polymere Dresden.
42. Bismarck, A., Kumru, M.E., Song, B., Springer, J., Moos, E. and Karger-Kocsis, J. (1999). Study on Surface- and Mechanical Fiber Characteristics and their Effect on the Adhesion Properties to a Polycarbonate Matrix Tuned by Anodic Carbon Fiber Oxidation, *Composites A*, **30**: 1351.
43. Meretz, S., Auersch, W., Marotzke, C., Schulz, E. and Hampe, A. (1993). Investigation of Morphology-Dependent Fracture-Behavior with the Single-Fiber Pull-Out Test, *Composites Sci. Technol.*, **48**: 285.
44. Marotzke, C. and Qiao, L. (1997). Interfacial Crack Propagation Arising in Single-Fiber Pull-Out Tests, *Composite Sci. Technol.*, **57**: 965.
45. Pisanova, E., Zhandarov, S., Mäder, E., Ahmad, I. and Young, R.J. (2001). Three Techniques of Interfacial Bond Strength Estimation from Direct Observation of Crack Initiation and Propagation in Polymer-fibre Systems, *Composites: Part A*, **32:** 435.
46. Subramanian, R.V., Jakubowski, J.J. and Williams, F.D. (1978). Interfacial Aspects of Polymer Coating by Electropolymerization, *J. Adhesion*, **9**: 185.